



Analytical analysis of multi-pulse NMR

Irina Nazarova, Marcus A. Hemminga*

Laboratory of Biophysics, Wageningen University, Dreijenlaan 3, 6703 HA Wageningen, The Netherlands

Received 20 January 2004; revised 17 May 2004

Available online 7 August 2004

Abstract

It is well known that in multi-pulse applications in high-resolution NMR and MRI a steady state is reached for the magnetisation vector by the effect of relaxation in combination with the pulse repetition time. In this paper, a mathematical model is developed to understand how the parameters of the pulse sequence and relaxation times T_1 and T_2 affect the behaviour of the magnetisation vector. It will be shown that even under strong simplifying conditions an analytical analysis becomes very complex and only an analytical solution can be found for 90° pulses and $T_1 = T_2$. For other cases a numerical approach is needed. Nevertheless, the basic approach of the mathematical analysis provides a general tool for analytical multi-operator applications. Our results provide a quantitative insight in the process by which the magnetisation relaxes towards the steady-state situation in a multi-pulse sequence.

© 2004 Elsevier Inc. All rights reserved.

Keywords: Analytical expression; Magnetisation vector; Pulse sequence; NMR relaxation; Homogeneous coordinates

1. Introduction

The problem of repeated RF pulses has been the subject of several investigations described in the literature. Freeman and Hill [1] solved the Bloch equations for such a case in high-resolution NMR, assuming a steady-state situation for the magnetisation. Waldstein and Wallace [2] extended Freeman and Hill's work and Meakin and Jesson [3] simulated a variety of multi-pulse and Fourier transform NMR experiments using a computer program based on the Bloch equations. Adler and Yeung [4] extended this work later, using the method of projection operators. Recently, Randall and co-worker [5] looked at the problem in the context of stray field magnetic resonance imaging (STRAFI) and in addition, it is an important part of Blumich's NMR Mouse [6].

Similar work has also come up in the analysis of CPMG sequences and chemical exchange [7], which is now being widely applied in the field of biomolecular NMR [8–10]. Also recently there has been an increasing interest in the use of steady-state free precession (SSFP) pulse sequences in fast scan MRI [11–13]. SSFP is also based on a sequence of closely spaced radiofrequency pulses, so that a steady-state signal is formed [14].

In this paper, we will re-examine this problem with the goal to explore the general mathematics related to multi-pulse sequences and to achieve an analytical calculation to get a systematic relationship between the parameters that describe the motion of the magnetisation vector during the pulse sequence. It will be shown that even under strong simplifying conditions an analytical analysis becomes very complex. Nevertheless, the basic approach of the mathematical analysis is elegant and provides a general tool for analytical multi-operator applications. Our results provide a quantitative insight in the process by which the magnetisation relaxes towards the steady-state situation in a multi-pulse sequence.

* Corresponding author. Fax: +31-317-482725.

E-mail address: marcus.hemminga@wur.nl (M.A. Hemminga).

URL: <http://ntmf.mf.wau.nl/hemminga/>.

2. Theory

Let us apply a series of equidistant pulses with a repetition time τ at times $0, \tau, 2\tau, \dots, n\tau$ (see Fig. 1). Each pulse rotates the magnetisation vector \mathbf{M} over an angle α around the x -axis of a rotating frame of reference $\{x, y, z\}$. We will neglect out-of-resonance effects of the applied radiofrequency field, so that the effective radiofrequency field is always directed along the x -axis. Also, relaxation during the pulses is neglected.

At the start of the pulse sequence, the magnetisation vector \mathbf{M} is along the z -axis and can be represented by

$$\mathbf{M}_0 = M_0 \begin{bmatrix} 0 \\ 0 \\ 1 \end{bmatrix}, \quad (1)$$

where M_0 is the equilibrium magnetisation.

Between the pulses the magnetisation vector \mathbf{M} precesses freely through an angle $\theta = \Delta\omega_0\tau$ around the z -axis, where $\Delta\omega_0$ is the offset from exact resonance with the radiofrequency. At the end of the free precession just before the next pulse the magnetisation vector can be described by [1]

$$\mathbf{M}_n = \mathbf{R}_z(\theta)\mathbf{S}(\tau, T_1, T_2)\mathbf{R}_x(\alpha)\mathbf{M}_{n-1} + (1 - E_1)\mathbf{M}_0 \quad (n \geq 1), \quad (2)$$

where

$$\mathbf{R}_x(\alpha) = \begin{bmatrix} 1 & 0 & 0 \\ 0 & \cos \alpha & \sin \alpha \\ 0 & -\sin \alpha & \cos \alpha \end{bmatrix}, \quad \mathbf{R}_z(\theta) = \begin{bmatrix} \cos \theta & \sin \theta & 0 \\ -\sin \theta & \cos \theta & 0 \\ 0 & 0 & 1 \end{bmatrix},$$

$$\mathbf{S}(\tau, T_1, T_2) = \begin{bmatrix} E_2 & 0 & 0 \\ 0 & E_2 & 0 \\ 0 & 0 & E_1 \end{bmatrix} \quad \text{and} \quad \begin{matrix} E_1 = \exp(-\tau/T_1) \\ E_2 = \exp(-\tau/T_2) \end{matrix}.$$

T_1 and T_2 are the spin–lattice and spin–spin relaxation times, respectively.

In principle Eq. (2) fully describes the magnetisation vector throughout the pulse sequence, but the problem

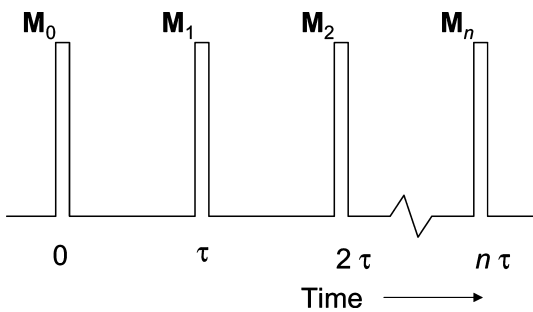


Fig. 1. Schematic illustration of the pulse sequence used in the analytical analysis. The sequence consists of a series of equidistant pulses at times $0, \tau, 2\tau, \dots, n\tau$, applied along the x -axis of a rotating frame of reference $\{x, y, z\}$. Actually the pulses are assumed to be extremely sharp. \mathbf{M}_n is the magnetisation vector just before each pulse is applied.

is that there is not a single matrix transformation from \mathbf{M}_0 to \mathbf{M}_n , without expressing \mathbf{M}_n from \mathbf{M}_{n-1} . This arises from the vector summation in Eq. (2). This problem can be solved by working in homogeneous coordinates, which enables us to combine both rotations and translations in one matrix transformation [15,16] (see Appendix A). Therefore, we move from 3×3 Cartesian coordinates to a 4×4 representation in homogeneous coordinates. This now allows a compact representation of the combined operators, which directly connects \mathbf{M}_0 and \mathbf{M}_n :

$$\mathbf{M}_n = \mathbf{A}^n \mathbf{M}_0. \quad (3)$$

Here the operator \mathbf{A} is given by

$$\mathbf{A} = \begin{bmatrix} E_2 \cos \theta & E_2 \cos \alpha \sin \theta & E_2 \sin \alpha \sin \theta & 0 \\ -E_2 \sin \theta & E_2 \cos \alpha \cos \theta & E_2 \sin \alpha \cos \theta & 0 \\ 0 & -E_1 \sin \alpha & E_1 \cos \alpha & 1 - E_1 \\ 0 & 0 & 0 & 1 \end{bmatrix} \quad (4)$$

and \mathbf{M}_0 is now expressed as

$$\mathbf{M}_0 = M_0 \begin{bmatrix} 0 \\ 0 \\ 1 \\ 1 \end{bmatrix}. \quad (5)$$

The challenge now is to find a general mathematical expression for \mathbf{A}^n . This is done in the following way [17]. Let matrix $\mathbf{\Lambda} = \mathbf{B}^{-1} \mathbf{A} \mathbf{B}$ be the diagonal form of matrix \mathbf{A} with diagonal values λ_1 to λ_4 which are the roots of the characteristic equation of matrix \mathbf{A} . Then

$$\mathbf{A}^n = \mathbf{B} \mathbf{\Lambda}^n \mathbf{B}^{-1}, \quad (6)$$

where $\mathbf{\Lambda}^n$ has a simple form with diagonal values λ_1^n to λ_4^n .

In general it turns out that polynomial equations with a degree >2 must be solved in the matrix inversion. This enormously increases the mathematical complexity, or is not feasible at all. Therefore, to keep the calculations manageable, we need to confine ourselves to a special case for which $\alpha = 90^\circ$ and $T_1 = T_2 = T$, so that $E_1 = E_2 = E$. In this case operator \mathbf{A} reduces to

$$\mathbf{A} = \begin{bmatrix} E \cos \theta & 0 & E \sin \theta & 0 \\ -E \sin \theta & 0 & E \cos \theta & 0 \\ 0 & -E & 0 & 1 - E \\ 0 & 0 & 0 & 1 \end{bmatrix}. \quad (7)$$

The calculation of λ_1 to λ_4 , \mathbf{B} and \mathbf{B}^{-1} is tedious, but straightforward. Since matrix \mathbf{A} is not Hermitian, the inverse of \mathbf{B} is not simply its adjoint, but must be calculated explicitly. The resulting matrix \mathbf{A}^n is given in Appendix B.

At this point, we make an inverse transformation from homogeneous coordinates to 3×3 Cartesian coordinates.

dinates to obtain an analytical representation for \mathbf{M}_n . This gives:

$$\mathbf{M}_n = \mathbf{M}_\infty + E^n \mathbf{F}_n. \tag{8}$$

In this equation \mathbf{M}_∞ is the steady-state magnetisation vector, which is given by

$$\mathbf{M}_\infty = \frac{M_0}{E^2 + 2E\gamma + 1} \begin{bmatrix} 2E\sqrt{\gamma(1-\gamma)} \\ E - 2E\gamma - E^2 \\ 1 - E + 2E\gamma \end{bmatrix}. \tag{9}$$

This steady-state magnetisation agrees with the results published by Freeman and Hill [1]. Vector \mathbf{F}_n represents the amplitude of the fluctuations around the equilibrium state and is given by

$$\mathbf{F}_n = \frac{(-1)^n EM_0}{E^2 + 2E\gamma + 1} \begin{pmatrix} \begin{bmatrix} -2\sqrt{\gamma(1-\gamma)} \\ E + 2\gamma - 1 \\ E + 1 \end{bmatrix} \sum_{k=0}^{\lfloor \frac{n}{2} \rfloor} \gamma^{n-2k} (\gamma^2 - 1)^k C_n^{2k} \\ + \begin{bmatrix} -2\sqrt{\gamma(1-\gamma)}(\gamma + E) \\ -(1-\gamma)(E + 2\gamma + 1) \\ -(1-\gamma)(1-E) \end{bmatrix} \sum_{k=0}^{\lfloor \frac{n-1}{2} \rfloor} \gamma^{n-2k-1} (\gamma^2 - 1)^k C_n^{2k+1} \end{pmatrix}. \tag{10}$$

In Eqs. (9) and (10) we have made the substitution

$$\gamma = \frac{1 - \cos \theta}{2}. \tag{11}$$

Furthermore, the brackets $[\dots]$ indicate integer values and

$$C_n^m = \frac{n!}{(n-m)!m!}$$

is the combinatorial coefficient.

3. Computational results

Calculations were performed on Eq. (8) using MATLAB 6.0. In analysing the behaviour of the magnetisation vector \mathbf{M}_n in Eq. (8), it is interesting to consider a plane, which is perpendicular to the steady-state vector \mathbf{M}_∞ and contains the end point of this vector. This plane is given by the equation

$$2E\sqrt{\gamma(1-\gamma)}x + (1 - 2E\gamma - E^2)y + (1 - E + 2E\gamma)z - \frac{M_0}{E^2 + 2E\gamma + 1} (4E^2\gamma^2 + 4E\gamma(E^2 - E + 1) + (E^2 + 1)(1 - E)^2) = 0. \tag{12}$$

Let us denote the end points of the magnetisation vector \mathbf{M}_n by P_n . From our calculations it follows that all points P_n are located approximately on the plane given by Eq. (12) (see Fig. 2). In all cases the deviation between the end points P_n and the plane is small ($\leq 10\%$) and decays during the pulse sequence with relaxation time $T = T_1 = T_2$. It should be noted from Eqs. (9) and

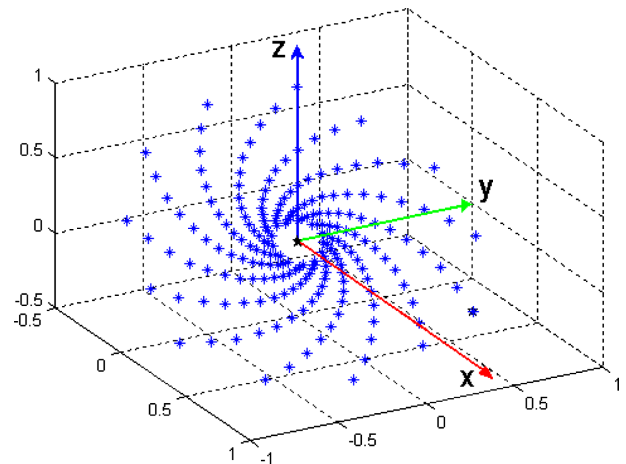


Fig. 2. Location of the end points P_n of the magnetisation vector \mathbf{M}_n during the pulse sequence for $E = 0.99$ and $\theta = 72^\circ$. The star indicates the end point of the equilibrium magnetisation vector \mathbf{M}_∞ , which is directed to the observer. All end points P_n are located on a spiral curve, which starts at \mathbf{M}_0 and ends in \mathbf{M}_∞ . This spiral curve is approximately in the plane given by Eq. (12), which is perpendicular to vector \mathbf{M}_∞ . This deviation is less than 10%. Both parameters E and θ (i.e., γ) influence the orientation of this plane. Parameter E has an influence on the speed of convergence of the points to the equilibrium point. The smaller E , the faster is the spiral convergence. Parameter θ defines the angle of rotation after each pulse around the spiral centre. In this plot \mathbf{M}_0 is normalised to 1. The number of pulses $n = 200$.

(12) that both parameters E and θ (i.e., γ) influence the orientation of the plane in the axes system $\{x, y, z\}$.

In all situations for $E < 1$, the length of the magnetisation vector \mathbf{M}_n will decrease during the pulse sequence due to the effect of relaxation and the end points P_n are found to be located on a spiral curve, which goes to the equilibrium point \mathbf{M}_∞ . This effect is illustrated in Fig. 3. The effect of parameter E , i.e., relaxation time T , is that it has an influence on the speed of convergence of the end points P_n to the equilibrium point. The smaller parameter E , the faster is the spiral convergence. Param-

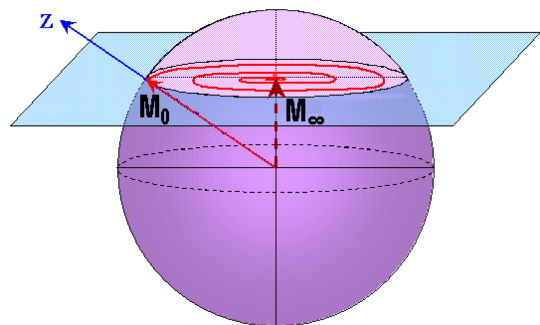


Fig. 3. Schematic illustration of the directions of the magnetisation vector \mathbf{M}_n during the pulse sequence for $E < 1$. \mathbf{M}_0 is the starting direction; \mathbf{M}_∞ is the equilibrium vector. All end points \mathbf{M}_n are located on a spiral, which starts at \mathbf{M}_0 (oriented along the z -axis) and ends in \mathbf{M}_∞ . The plane given by Eq. (12), which contains the spiral, is perpendicular to the equilibrium vector \mathbf{M}_∞ and contains the end point of this vector.

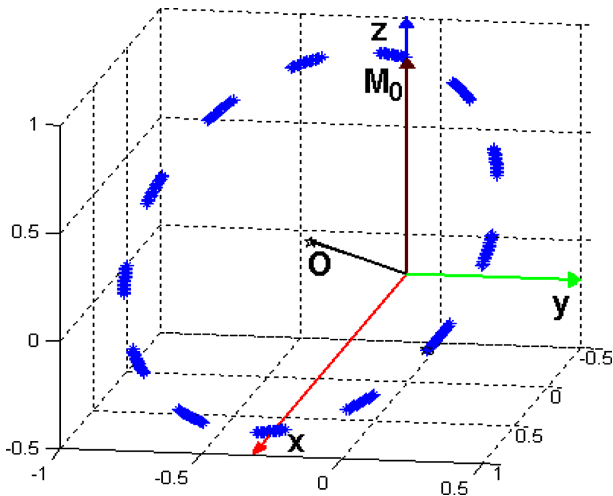


Fig. 4. Location of the end points P_n of the magnetisation vector \mathbf{M}_n during the pulse sequence in the case of no relaxation ($E = 1$) and $\theta = 73^\circ$. All end points P_n are located exactly on a circle given by Eqs. (14) and (15). The star denotes the end point of vector \mathbf{O} (see Eq. (14)). The plane given by Eq. (13), which contains the circle, is perpendicular to \mathbf{M} and contains the end point of this vector. In this plot \mathbf{M}_0 is normalised to 1. The number of pulses $n = 200$.

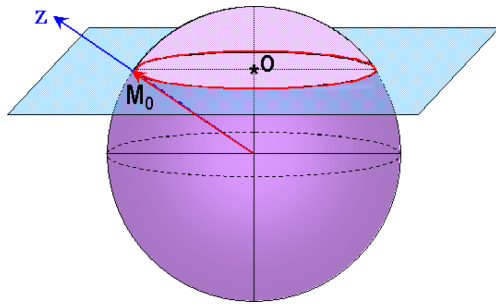


Fig. 5. Schematic illustration of the directions of the magnetisation vector \mathbf{M}_n during the pulse sequence in the case of no relaxation ($E = 1$). \mathbf{M}_0 is the starting direction, which is along the z -axis. The star denotes the end point of vector \mathbf{O} (see Eq. (14)). The length of the magnetisation vector \mathbf{M}_n does not change in time, so all end points of this vector stay on the circle on the plane given by Eq. (13). The system never reaches an equilibrium state.

eter θ defines the angle of rotation after each pulse around the spiral centre.

In the special case of no relaxation, i.e., for $E = 1$, it can be demonstrated that all end points P_n are located exactly on a circle in the plane, which follows from Eq. (12):

$$\sqrt{\gamma(1-\gamma)}x - \gamma y + \gamma z - \gamma M_0 = 0. \quad (13)$$

This plane is perpendicular to the vector

$$\mathbf{O} = \frac{M_0}{1+\gamma} \begin{bmatrix} \sqrt{\gamma(1-\gamma)} \\ -\gamma \\ \gamma \end{bmatrix} \quad (14)$$

and contains the end point of this vector as well as \mathbf{M}_0 . This circle has a radius

$$r = \frac{M_0}{\sqrt{1+\gamma}} \quad (15)$$

and a centre in the end point given by Eq. (14). This is illustrated in Figs. 4 and 5.

4. Discussion

The aim of this paper is to obtain an analytical expression for the magnetisation vector during a pulse sequence. In our analysis the magnetisation vector \mathbf{M}_n is followed by taking ‘‘snapshots’’ just before the pulses are given (Fig. 1). In fact this reduces to the problem of finding an expression for \mathbf{A}^n (see Eq. (3)), which is done by getting a diagonal representation for the transformation operator \mathbf{A} (Eq. (6)). Basically this is an attractive method to find the result of a multi-operator calculation, such as appear in multi-pulse NMR experiments. Although the calculation in Eq. (3) could be carried out using a numerical algorithm, an analytical expression has the advantage of giving the relationships between the different parameters in an NMR experiment. Getting a diagonal representation for the transformation operator \mathbf{A} is only possible, however, for a relatively simple form of \mathbf{A} . This is related to the fact that finding roots analytically is only manageable for linear and quadratic equations. In our case, therefore, we had to limit ourselves to 90°_x pulses and relaxation time $T = T_1 = T_2$. This situation refers to an NMR experiment on a mobile liquid sample.

Under these conditions, the time dependency of the magnetisation vector takes a simple general form of relaxation towards an equilibrium state (Eq. (8)). The relaxation time T forces the magnetisation vector to relax to the steady-state situation given by \mathbf{M}_∞ and the time-dependent fluctuations decay with time to zero with the factor $E^n = \exp(-n\tau/T)$.

As is schematically shown in Fig. 3, the relaxation process can be described by a spiral trajectory from the starting magnetisation vector \mathbf{M}_0 to the steady-state vector \mathbf{M}_∞ , with end points of the magnetisation vector \mathbf{M}_n roughly in a plane that is located perpendicular to \mathbf{M}_∞ and contains the end point of \mathbf{M}_∞ . However, in the case that there is no relaxation, the length of magnetisation vector \mathbf{M}_n is constant and equal to M_0 (Fig. 5). Therefore the magnetisation is confined to a circular path at the outline of the spiral on a cone with symmetry axis given by vector \mathbf{O} (which is \mathbf{M}_∞ for $E = 1$). Since the length of the magnetisation vector does not change in time, the system never does reach an equilibrium state, as would be expected in this case.

For other cases that T_1 and T_2 are not equal (but note that $T_1 \geq T_2$), it can be numerically calculated from Eq. (3) that the plane on which the end points P_n are located deforms into a concave surface with a symmetry

axis given by \mathbf{M}_∞ . This indicates that due to the relaxation processes there always is a strong driving force, which constantly forces the magnetisation vector \mathbf{M}_n to be parallel to \mathbf{M}_∞ .

Acknowledgment

We wish to thank Dr. M.H. Hendriks from the Mathematical and Statistical Methods Group, Wageningen University, for his valuable advice.

Appendix A. Homogeneous coordinates

Homogeneous coordinates are used if one wants to combine rotations, scaling, and translations in *one* matrix transformation. An extra coordinate is introduced to take into account the non-linearities. Homogeneous coordinates are derived from Cartesian coordinates as follows:

$$\begin{bmatrix} x \\ y \\ z \end{bmatrix}_{\text{Cart}} \Rightarrow \begin{bmatrix} x \\ y \\ z \\ 1 \end{bmatrix}_{\text{hom}},$$

where (x, y, z) is a vector in Cartesian coordinates. To map an arbitrary vector (x, y, z, w) , $w \neq 0$ in homogeneous coordinates back to a vector in Cartesian coordinates, we divide the first three terms by the fourth (w) term. Thus

$$\begin{bmatrix} x \\ y \\ z \\ w \end{bmatrix}_{\text{hom}} \Rightarrow \begin{bmatrix} x/w \\ y/w \\ z/w \end{bmatrix}_{\text{Cart}}.$$

To show the fundamental nature of homogeneous coordinates, we will illustrate its application on a translation operation. A translation in Cartesian coordinates by (t_x, t_y, t_z) is a sum of two vectors:

$$\begin{bmatrix} x \\ y \\ z \end{bmatrix} + \begin{bmatrix} t_x \\ t_y \\ t_z \end{bmatrix} = \begin{bmatrix} x + t_x \\ y + t_y \\ z + t_z \end{bmatrix}.$$

This operation cannot be represented as a product of multiplication of the initial vector and a 3×3 transformation matrix. But if we add one more coordinate to this vector, the transformation matrix \mathbf{T} for this translation will have the following form:

$$\mathbf{T}(t_x, t_y, t_z) = \begin{bmatrix} 1 & 0 & 0 & t_x \\ 0 & 1 & 0 & t_y \\ 0 & 0 & 1 & t_z \\ 0 & 0 & 0 & 1 \end{bmatrix}$$

and the translation operation can be easily represented as a product of multiplication:

$$\begin{bmatrix} 1 & 0 & 0 & t_x \\ 0 & 1 & 0 & t_y \\ 0 & 0 & 1 & t_z \\ 0 & 0 & 0 & 1 \end{bmatrix} \begin{bmatrix} x \\ y \\ z \\ 1 \end{bmatrix} = \begin{bmatrix} x + t_x \\ y + t_y \\ z + t_z \\ 1 \end{bmatrix}.$$

In a similar way, we can define and apply the transformations for scaling and rotation, as given below.

The transformation matrix of a scaling operation \mathbf{S} is:

$$\mathbf{S}(s_x, s_y, s_z) = \begin{bmatrix} s_x & 0 & 0 & 0 \\ 0 & s_y & 0 & 0 \\ 0 & 0 & s_z & 0 \\ 0 & 0 & 0 & 1 \end{bmatrix}.$$

The matrix of rotation \mathbf{R} about the x , y , and z -axis by α has the following form:

$$\mathbf{R}_x(\alpha) = \begin{bmatrix} 1 & 0 & 0 & 0 \\ 0 & \cos \alpha & \sin \alpha & 0 \\ 0 & -\sin \alpha & \cos \alpha & 0 \\ 0 & 0 & 0 & 1 \end{bmatrix},$$

$$\mathbf{R}_y(\alpha) = \begin{bmatrix} \cos \alpha & 0 & -\sin \alpha & 0 \\ 0 & 1 & 0 & 0 \\ \sin \alpha & 0 & \cos \alpha & 0 \\ 0 & 0 & 0 & 1 \end{bmatrix},$$

$$\mathbf{R}_z(\alpha) = \begin{bmatrix} \cos \alpha & \sin \alpha & 0 & 0 \\ -\sin \alpha & \cos \alpha & 0 & 0 \\ 0 & 0 & 1 & 0 \\ 0 & 0 & 0 & 1 \end{bmatrix}.$$

In conclusion, homogeneous coordinates unify the treatment of common graphical transformations and operations. This allows a compact representation of the combined operations that is easy to apply. In homogeneous coordinates the sequential execution of any combination of all three types of operations gives one matrix, which can be presented as a product of matrixes of the corresponding transformations. The result of multiplication of any number of matrixes of \mathbf{T} , \mathbf{S} , and \mathbf{R} is always of the following form:

$$\begin{bmatrix} r_{11} & r_{12} & r_{13} & t_x \\ r_{21} & r_{22} & r_{23} & t_y \\ r_{31} & r_{32} & r_{33} & t_z \\ 0 & 0 & 0 & 1 \end{bmatrix}.$$

Here the 3×3 upper left part of the matrix determines the resulting rotation and scaling, and the three coefficients of the 4th column determine the resulting translation.

Appendix B. Matrix A^n

We make the following substitutions (γ is given in Eq. (11)):

$$\sigma_{\pm} = \frac{1}{2}\sqrt{2}(\sqrt{1-\gamma} \pm i\sqrt{1+\gamma})$$

and

$$W = \frac{1}{E^2 + 2E\gamma + 1}.$$

Then matrix A^n can be written in the following way:

$$A^n = W \begin{bmatrix} 0 & 0 & 0 & 2E\sqrt{\gamma(1-\gamma)} \\ 0 & 0 & 0 & E - 2E\gamma - E^2 \\ 0 & 0 & 0 & 1 - E + 2E\gamma \\ 0 & 0 & 0 & 1/W \end{bmatrix} + \frac{E^n}{1+\gamma} \begin{bmatrix} (1-\gamma) + \gamma(\sigma_+^{2n} + \sigma_-^{2n}) \\ -\sqrt{\gamma(1-\gamma)} + \frac{1}{2}\sqrt{2\gamma}(\sigma_+^{2n+1} + \sigma_-^{2n+1}) \\ \sqrt{\gamma(1-\gamma)} - \frac{1}{2}\sqrt{2\gamma}(\sigma_+ \sigma_-^{2n} + \sigma_+^{2n} \sigma_-) \\ 0 \end{bmatrix} \dots \begin{bmatrix} -\sqrt{\gamma(1-\gamma)} + \frac{1}{2}\sqrt{2\gamma}(\sigma_+ \sigma_-^{2n} + \sigma_+^{2n} \sigma_-) \\ \gamma + \frac{1}{2}(\sigma_+^{2n} + \sigma_-^{2n}) \\ -\gamma - \frac{1}{2}(\sigma_+^2 \sigma_-^{2n} + \sigma_+^{2n} \sigma_-^2) \\ 0 \end{bmatrix} \dots \begin{bmatrix} \sqrt{\gamma(1-\gamma)} - \frac{1}{2}\sqrt{2\gamma}(\sigma_+^{2n+1} + \sigma_-^{2n+1}) \\ -\gamma - \frac{1}{2}(\sigma_+^{2n+2} + \sigma_-^{2n+2}) \\ \gamma + \frac{1}{2}(\sigma_+^{2n} + \sigma_-^{2n}) \\ 0 \end{bmatrix} \dots \begin{bmatrix} -\sqrt{\gamma(1-\gamma)} + \frac{1}{2}W\sqrt{2\gamma}(E-1)\{(\sigma_-E - \sigma_+) \sigma_+^{2n} + (\sigma_+E - \sigma_-) \sigma_-^{2n}\} \\ \gamma + \frac{1}{2}W(E-1)\{(\sigma_-E - \sigma_+) \sigma_+^{2n+1} + (\sigma_+E - \sigma_-) \sigma_-^{2n+1}\} \\ -\gamma - \frac{1}{2}W(E-1)\{(\sigma_-E - \sigma_+) \sigma_+^{2n} \sigma_- + (\sigma_+E - \sigma_-) \sigma_+ \sigma_-^{2n}\} \\ 0 \end{bmatrix}.$$

The first part is a stationary part (independent of n) and the second part is time time-dependent (i.e., a function of n).

References

- [1] R. Freeman, H.D.W. Hill, Phase and intensity anomalies in Fourier transform NMR, *J. Magn. Reson.* 4 (1971) 366–383.
- [2] P. Waldstein, W.E. Wallace Jr., Driven equilibrium methods for enhancement of nuclear transients, *Rev. Sci. Instr.* 42 (1971) 437–440.
- [3] P. Meakin, J.P. Jesson, Computer simulation of multipulse and Fourier transform NMR experiments. I. Simulations using the Bloch equations, *J. Magn. Reson.* 10 (1973) 290–315.
- [4] R.S. Adler, H.Y. Yeung, Transient decay of longitudinal magnetisation in heterogeneous spin systems under selective saturation. III. Solution by projection operators, *J. Magn. Reson. A* 104 (1993) 321–330.
- [5] A.D. Bain, E.W. Randall, Hahn spin echoes in large static gradients following a series of 90° pulses, *J. Magn. Reson. A* 123 (1996) 49–55.
- [6] G. Eidmann, R. Savelsberg, P. Blümmler, B. Blümich, The NMR MOUSE: a mobile universal surface explorer, *J. Magn. Reson. A* 122 (1996) 104–109.
- [7] J.P. Carver, R.E. Richards, A general two-site solution for the chemical exchange produced dependence of T_2 upon the Carr–Purcell pulse separation, *J. Magn. Reson.* 6 (1972) 89–105.
- [8] J.P. Loria, M. Rance, A.G. Palmer, A relaxation-compensated Carr–Purcell–Meiboom–Gill sequence for characterizing chemical exchange by NMR spectroscopy, *J. Am. Chem. Soc.* 121 (1999) 2331–2332.
- [9] N.R. Skrynnikov, F.A. Mulder, B. Hon, F.W. Dahlquist, L.E. Kay, Probing slow time scale dynamics at methyl-containing side chains in proteins by relaxation dispersion NMR measurements: application to methionine residues in a cavity mutant of T4 lysozyme, *J. Am. Chem. Soc.* 123 (2001) 4556–4566.
- [10] N.R. Skrynnikov, F.W. Dahlquist, L.E. Kay, Reconstructing NMR spectra of “invisible” excited protein states using HSQC and HMQC experiments, *J. Am. Chem. Soc.* 124 (2002) 12352–12360.
- [11] W. Hänicke, H.U. Vogel, An analytical solution for the SSFP signal in MRI, *Magn. Reson. Med.* 49 (2003) 771–775.
- [12] P. Le Roux, Simplified model and stabilization of SSFP sequences, *J. Magn. Reson.* 163 (2003) 23–37.
- [13] B.A. Hargreaves, S.S. Vasanawala, K.S. Nayak, B.S. Hu, D.G. Nishimura, Fat-suppressed steady-state free precession imaging using phase detection, *Magn. Reson. Med.* 50 (2003) 210–213.
- [14] M.L. Gyngell, The steady-state signals in short-repetition-time sequences, *J. Magn. Reson.* 81 (1989) 474–483.
- [15] Standard Mathematical Tables and Formulae, 30th ed., CRC Press, Boca Raton, 1996.
- [16] M. Helgstrand, T. Härd, P. Allard, Simulations of NMR pulse sequences during equilibrium and non-equilibrium chemical exchange, *J. Biomol. NMR* 18 (2000) 49–63.
- [17] F.R. Gantmacher, The Theory of Matrices, vols. 1 and 2, Chelsea, New York, 1959 Translation of [18] by K.A. Hirsch.
- [18] F.R. Gantmacher, Teoriya matric, Gosudarstv. Izdat. Tehn.-Teor. Lit., Moscow, 1953 (in Russian).